

유전체 장벽 방전 전기적 특성의 폴리에틸렌 표면 개질에 대한 영향

Chuan He, Yongqian Wu, Erping Deng[†], Yawen Zhou*, Zhu Zhang, and Lijian Ding

School of Electrical Engineering and Automation, Hefei University of Technology

*School of Electrical Engineering, Xi'an Jiaotong University

(2023년 10월 24일 접수, 2023년 12월 10일 수정, 2023년 12월 11일 채택)

Influence of Dielectric Barrier Discharge Electrical Properties on the Surface Modification of Polyethylene

Chuan He, Yongqian Wu, Erping Deng[†], Yawen Zhou*, Zhu Zhang, and Lijian Ding

School of Electrical Engineering and Automation, Hefei University of Technology, Hefei, Anhui, 230009, China

*School of Electrical Engineering, Xi'an Jiaotong University, Xi'an, Shanxi 710049, China

(Received October 24, 2023; Revised December 10, 2023; Accepted December 11, 2023)

Abstract: Dielectric barrier discharge (DBD) is a commonly used plasma surface modification technique, and the power parameters play a crucial role in influencing the modification results. Electrical properties of DBD pulses were studied by varying both power and frequency. Additionally, how these electrical properties influence the chemical and topographical alterations in polyethylene surface modification was investigated. In terms of chemical changes, we found that higher power supply significantly enhances the modification result, whereas alterations in frequency do not exert a substantial impact. Concerning topographical changes, increased power supply yielded similarly effective results, while heightened supply frequency improved the modification result due to the enhanced uniformity of discharge pulses. Regarding hydrophobicity, power supply exerts a more significant and pronounced influence compared to frequency.

Keywords: plasma, electrical properties, polyethylene, surface modification.

Introduction

Polymers, known for their impressive thermal and mechanical properties, have extensive applications across various industries, including medical devices, automotive, chemicals, electronics engineering, and more.¹⁻⁴ The surface properties of polymers, including roughness and hydrophobicity, significantly impact their applications.⁵⁻⁷ Consequently, in today's context, the focus extends beyond material synthesis to surface modifications.

Among the prominent surface modification techniques, plasma surface modification stands out. It is commonly used for tasks such as cleaning, etching, cross-linking, and surface activation.⁸⁻¹⁰ One notable method is dielectric barrier discharge (DBD), a plasma discharge technique that generates ions and electrons

by breaking down the electric field within an insulating medium. This process results in a uniform and stable plasma at atmospheric pressure. Within the critical outermost layer of the material, it interacts with the primary polymer or oligomers, leading to the formation of new functional groups or alterations in physical topography.¹¹⁻¹⁸ This transformation is typically confined to the material's surface, preserving its intrinsic properties and offering precise control over surface modification. DBD stands out among various plasma discharge methods, such as corona and arc discharges, due to the presence of insulating dielectrics on the electrode surface or within the discharge area. In a typical two-electrode configuration, the intense electric field within the discharge zone triggers gas ionization. Resultantly, charged particles migrate to the surface of the insulating dielectric, generating an internal electric field opposing the externally applied field. This field curtails the escalation of the discharge, leading to its extinction, thereby averting a transition to arc or spark discharges and ensuring discharge stability. Consequently, DBD has gained widespread attention

[†]To whom correspondence should be addressed.
erpings.deng@hfut.edu.cn, ORCID[®]0000-0001-5047-0834
©2024 The Polymer Society of Korea. All rights reserved.

and application owing to its uncomplicated structure and stable discharge performance.¹⁹⁻²⁵

While previous research has predominantly explored the influence of various factors like reactive atmospheres and treatments on modification outcomes, there remains a dearth of studies examining the impact of the discharge power on these outcomes.²⁶⁻²⁹ In reality, the electrical properties of the DBD power directly determine the discharging intensity and energetic accumulation of plasma pulses. These factors constitute the energetic sources for surface modification and hold a pivotal role in shaping its effectiveness.³⁰⁻³⁹

Polyethylene, one of the world's five major general-purpose resin categories, stands out due to its remarkable mechanical properties, chemical stability, and cost-effectiveness. It enjoys widespread use in both industrial production and daily life. In this paper, using polyethylene as a case study, we delve into the electrical properties of DBD pulses and their influence on surface modification outcomes. Our objective is to unveil the underlying patterns connecting discharge electrical properties and modification results.

Experimental

Materials and Methods. **Materials:** The experimental materials and reagent specifications used in this research are shown in Table 1, wherein high-purity air was employed for the reaction atmosphere, and ethanol was used for cleaning the poly-

ethylene material.

Experimental Facilities. The experimental equipment used in research is as shown in Table 2, The power supply, oscilloscope, probes, and other equipment were employed for the discharge circuit. Fourier-transform infrared spectrometer was utilized for characterizing the functional groups on the polyethylene surface. Gas chromatography was employed for identifying reaction byproducts. Atomic force microscopy was used to characterize the surface topography and roughness of polyethylene. Contact angle measurement equipment was used to measure the hydrophobicity of the polyethylene surface. A digital camera was utilized for capturing images of the plasma discharge.

DBD Principle of DBD: The experimental circuit principle is shown in Figure 1, the DBD method was chosen, grounding the plasma power output through a sampling capacitor through the reactor. Voltage measurements were obtained via a 470000 pF capacitor, while current measurements were acquired using a 50 Ω resistor. The discharge voltage and current waveforms were recorded across various plasma power parameters. The gas flow rate was maintained at 5 L/min, the atmosphere was experimental air, and the treatment duration was 40 seconds. The electrode diameter is 100 mm, with an 8 mm discharge interval.

Analysis of DBD: Power and electrical properties can be analyzed through Lissajous figures. The derivation of discharge power is as follows: The transient discharge current I

Table 1. Materials and Reagents Used in the Experiment

Material/Reagent	Specifications	Manufacturer
Polyethylene Sheet	Thickness: 0.50 mm, Density: 0.921 g/cm ³	Dongguan Xinda Yuan Insulation Materials, China, Co., Ltd.
Air (79% N ₂ , 21% O ₂)	Purity \geq 99.999%	Shenhe Gas, China, Co., Ltd.
Ethanol	Content: 99%	Suzhou Chenze Chemical, China, Co., Ltd.

Table 2. Instruments and Equipment Used in the Experiment

Instrument Name	Model/Specifications	Manufacturer
Plasma Power Supply	CTP-2000KP	Nanjing Suman tech Plasma Technology, China, Co., Ltd.
Oscilloscope	TDS2024C	Tektronix Technology, USA, Co., Ltd.
Probe	Tektronix P6015A	Tektronix Technology, USA, Co., Ltd.
Fourier Infrared Spectrometer	Nicolet 6700	Thermo Fisher, USA, Co., Ltd.
Gas Chromatograph	GC 1949	Changzhou Panuo Instrument, China, Co., Ltd.
Atomic Force Microscope	Dimension Icon	Bruker, Germany Co., Ltd.
Contact Angle Measurement Instrument	SDCA911031	Dongguan Shengding Precision Instrument, China, Co., Ltd.
Digital camera	EOS R50	Canon, Japan, Co., Ltd.

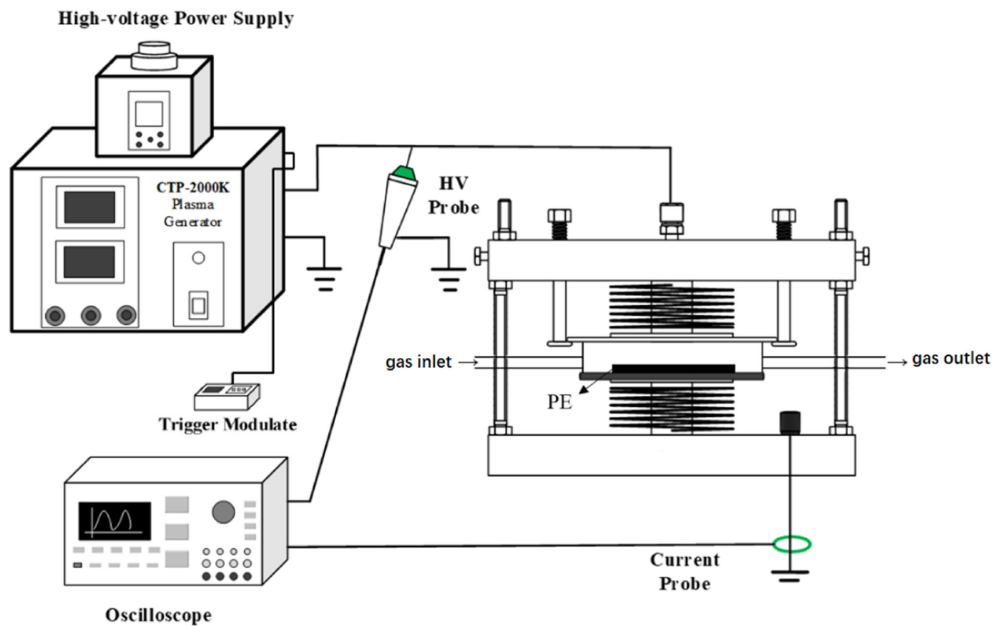


Figure 1. Schematic diagram of DBD experiment setup.

satisfies the formula:

$$I(t) = \frac{dQ}{dt} = C_M \frac{dU_c}{dt} \quad (1)$$

where t is the discharge time, Q is the charge measured by the capacitor, C_M is the capacitance connected in the circuit, which is the sampling capacitance, and U_c is the voltage across the capacitor.

Therefore, the discharge power (P_D) is given by:

$$P_D = \frac{1}{T} \int_0^T U(t) \times I(t) dt = f \times C_M \times S \quad (2)$$

where S represents the area enclosed by the Lissajous figure. T is the discharge period, and f is the power supply frequency.

The voltage and current waveforms obtained in the experiment are shown in Figure 2(a). By integrating the voltage and current, we obtain the integral values and plot the Lissajous figure as shown in Figure 2(b). The output frequency f is obtained from the oscilloscope reading. The internal sampling capacitance C_M of the power supply is $0.47 \mu\text{F}$, the voltage sampling ratio $k = 1000$, and both CH1 and CH2 signal channels use probes with attenuation factors of 1 (no attenuation, $k_x = k_y = 1$).

Hence, the actual discharge power is calculated using the following formula:

$$P = f \times C_M \times k \times k_x \times k_y \times S \quad (3)$$

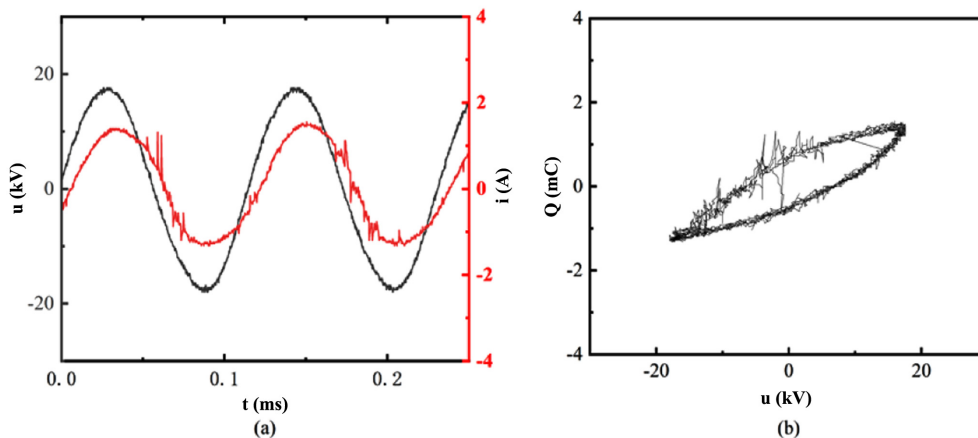


Figure 2. (a) Voltage-current waveforms; (b) lissajous figures.

The voltage-charge relationship, represented by Lissajous figures, and the equivalent circuit of DBD can be explained as follows: before the gap breakdown, DBD is equivalent to a series connection of the barrier dielectric equivalent capacitance C_d and the gap equivalent capacitance C_g . After gap breakdown, it is equivalent to a series connection of the barrier dielectric equivalent capacitance C_d and the plasma resistance R . The left and right sides of the Lissajous figure correspond to different discharge phases, while the top and bottom sides correspond to the cutoff stages of the discharge. The formulas for calculating the dielectric capacitance C_d , the gap capacitance C_g , and the total capacitance C_0 are as follows, where C_M is the sampling capacitance, and k is the voltage division ratio.

$$C_d = \frac{U_{c3}}{(U_{\max} - U_1) \times k} \times C_M \quad (4)$$

$$C_0 = \frac{U_{c2} - U_{c4}}{-U_{\max} \times k} \times C_M \quad (5)$$

$$C_g = \frac{C_0 \times C_d}{C_d - C_0} \quad (6)$$

It is evident that the dielectric capacitance is not constant under different discharge conditions. In fact, due to the lack of temperature control during the experimental process, the temperature of the dielectric sheets increases due to the significant heat generated by the plasma during discharge, leading to changes in the numerical value of the dielectric capacitance.

DBD Results: Under atmospheric pressure conditions, DBD exhibits two discharge modes: filamentary mode and uniform mode, with the filamentary mode being the most common. According to gas discharge theory, the mean free path of electrons λ_e in a gas is inversely proportional to the gas pressure p . Under atmospheric pressure, the mean free path of electrons is very short. Therefore, the number of collisions $N = d/\lambda_e$ experienced by electrons traveling from the cathode to the anode in a gap of distance d is proportional to pd , and the value of N will be very large. This leads to the development of intense electron avalanches in the discharge, resulting in the transition to a filamentary discharge mode.

$$U_g = U_a - U_d = U_a - \frac{1}{C_d} \int idt \quad (7)$$

Where U_a and U_d are the applied voltage and the voltage across the barrier dielectric, respectively. When the gap is broken, the current i increases rapidly, leading to a rapid accumulation of charge on the barrier dielectric surface and an increase in U_d .



Figure 3. Filamentary DBD observed in the experiment.

This, in turn, causes a decrease in U_g until the discharge extinguishes, inhibiting the formation of an arc. Therefore, during this experimental process, numerous small and transient discharge filaments can be observed randomly distributed within the reactor, as shown in Figure 3.

Polyethylene Treatment: To eliminate surface impurities and contaminants, the polyethylene sheets were cut into 50×50 mm dimensions. Subsequently, they were immersed in anhydrous ethanol for 4 hours, followed by a rinse with distilled water. After gentle drying at low temperatures, these pre-treated polyethylene samples were securely attached to metal sheets using adhesive tape and then placed inside the DBD reactor. To ensure airtightness, a 1mm-thick wet silicone gasket was applied around the reactor. Finally, the reactor was sealed with a 3 mm-thick quartz plate measuring 200 mm in diameter.

Once the circuit and gas connections have been confirmed correctly, the experiment is allowed to begin. Start by opening the gas cylinder valve and regulating the pressure with the pressure reducing valve to keep it within the appropriate range. Next, fine-tune the gas flow rate to 5L/min using the flowmeter knob. Wait for about 2 minutes to ensure the experimental gas completely fills the reaction apparatus. Adjust the regulator knob and determine the right input voltage by observing the waveform display. Fine-tune the output frequency using the adjustment knob, initiate the discharge, and set the resonance current to its maximum or designated value to kickstart the experiment. When you've completed the experiment, readjust the regulator knob to zero the power output voltage and switch off the control power supply.

Structural Characterization and Performance Testing: In order to investigate the changes in the surface properties of polyethylene after DBD surface modification, characterization was conducted from three aspects: surface chemical functional groups, microscale surface roughness, and hydrophilicity.

Fourier Infrared Spectroscopy: Fourier Infrared Spectroscopy was used to characterize the polar functional groups on the surface, revealing chemical changes resulting from sur-

face modification.

Product Analysis: Modified degradation products were analyzed using a gas chromatograph to confirm chemical changes resulting from surface modification.

Topographical Characterization: The surface topography of the modified material was observed using an atomic force microscope, enabling the acquisition of nanoscale surface topographical structures.

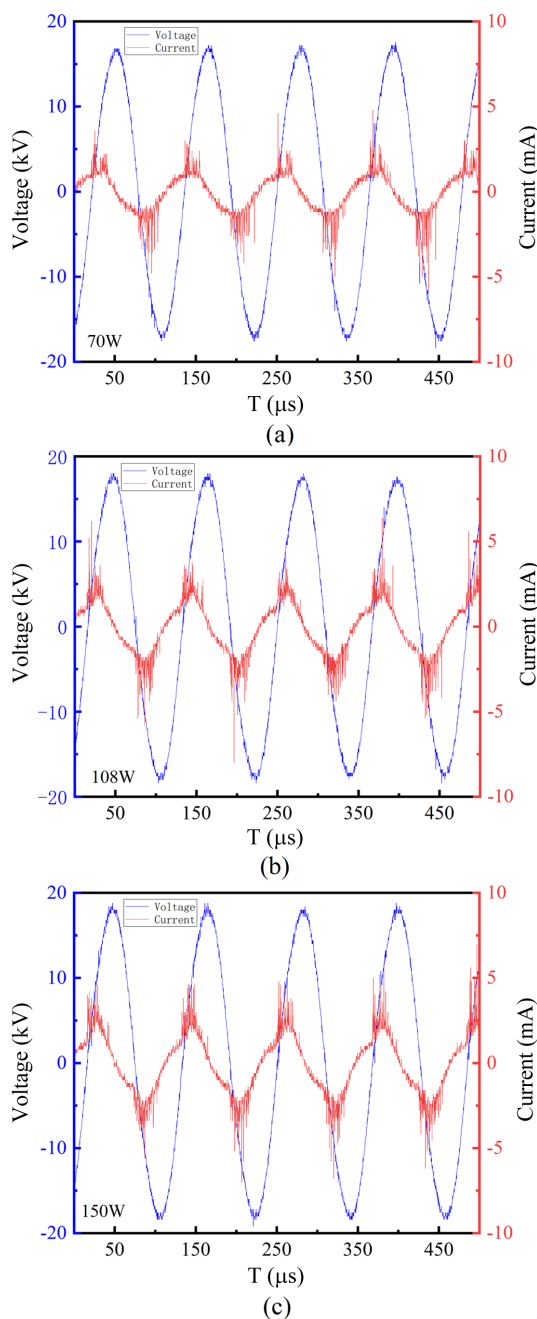


Figure 4. Discharge voltage-current waveforms at different powers: (a) 70 W; (b) 108 W; (c) 150 W.

Contact Angle Measurements: The Contact Angle Measurement Instrument is employed to measure the water contact angle (WCA) of the sample through fitting and analysis using image analysis software. By placing the treated polyethylene sheets in ambient air conditions (25 °C, 40% humidity) and subsequently measuring the water contact angle at various time intervals, the impact of placement duration on the hydrophilic properties of the material following plasma surface modification is investigated.

Results and Discussion

Impact of Power Parameters on DBD. **Impact of Different Powers on DBD:** In Figures 4(a), (b), and (c), the discharge voltage-current waveforms were depicted for power supply levels of 70, 108, and 150 W, respectively. These experiments were conducted with a gas flow rate of 5 L/min, experimental air conditions, and a 40-second treatment duration. Notably, as the power supply increased, a corresponding rise was observed in current amplitude. This can be attributed to the greater energy storage during the discharge process, resulting in heightened discharge current within the same timeframe.

Figure 5 displays the Q-V Lissajous diagrams, which validate our findings. Actuators effectively match the pulse source, resulting in well-enclosed Lissajous diagrams resembling parallelograms. Surface alternating discharge is introduced, which led to the elliptical shape. Notably, varying power supply levels have a limited impact on the Lissajous diagram shape, as all three diagrams exhibit similar shapes. However, increasing power supply correlated with higher transferred charge amplitudes—measuring 1.1, 1.3, and 1.6 mC respectively—highlighting the increased

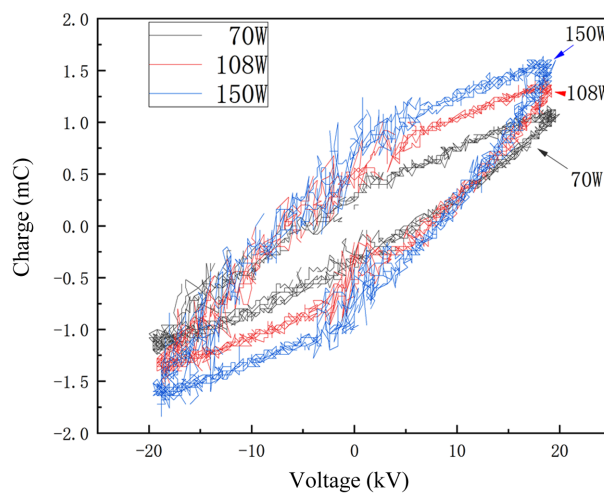


Figure 5. Comparison of lissajous diagrams at different powers.

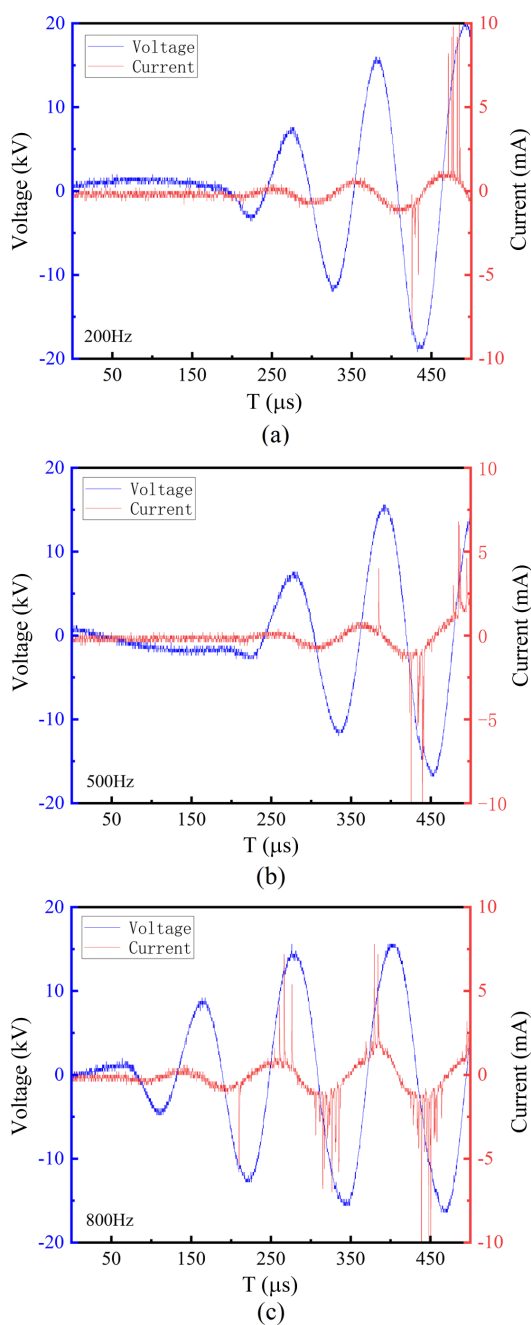


Figure 6. Discharge voltage-current waveforms at different frequencies: (a) 200 Hz; (b) 500 Hz; (c) 800 Hz.

transferring charge and energy with higher power supply.

Impact of Different Frequencies on DBD: Figures 6(a), (b), and (c) illustrated discharge voltage-current waveforms at supply frequencies of 200, 500, and 800 Hz, respectively. Under the conditions of a controlled gas flow rate of 5 L/min, experimental air, an actual discharge power of 70W, and a 40-second treatment duration, noteworthy trends emerged. As the

supply frequency increased, the discharge rate accelerated, yielding more discharges, yet each discharge's amplitude decreased. This phenomenon is attributed to the heightened frequency, which enhances dielectric recovery speed post-discharge, facilitating more extensive plasma diffusion within the discharge region, ultimately expediting the discharge process.

Examining the discharge outcomes via Figure 7's Lissajous diagrams, we note that the shapes and amplitudes across the three distinct supply frequencies share remarkable similarity and show no discernible pattern. This suggests that the influence of supply frequency on Lissajous diagrams is relatively minimal, and both pulse transferring charge and energy remain constant. Consequently, it's evident that pulse frequency significantly impacts the rate of energy accumulation during discharge, while discharge intensity remains unaffected.

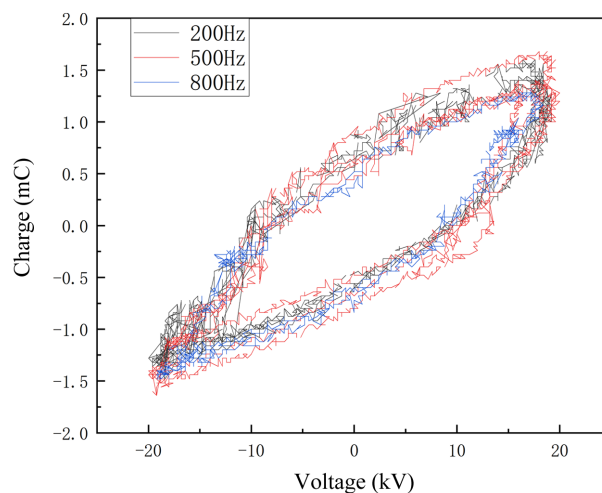


Figure 7. Comparison of lissajous diagrams at different frequencies.

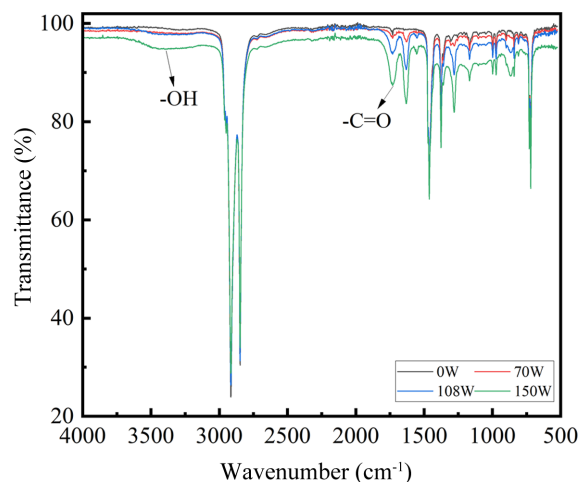


Figure 8. Infrared spectra of polyethylene surfaces after treatment at different discharge powers.

Chemical Changes Induced by DBD. In investigation of plasma surface treatment using various power supply parameters, the aim is to understand how these factors influence the treatment outcomes. Firstly, examine the infrared spectroscopy of polyethylene surfaces treated with DBD at different power levels. Our experimental conditions include a gas flow rate of 5L/min, experimental air, a discharge frequency of 200 Hz, and a treatment duration of 40 seconds.

As depicted in Figure 8, when applying power supply levels of 70, 108, and 150 W, new absorption peaks emerge on the polyethylene surface around 1500-1750 cm^{-1} and 3050-3500 cm^{-1} , corresponding to the -C=O and -OH functional groups. Notably, these peaks intensify as the discharge power increases. The -C=O and -OH groups exhibit the most pronounced changes. This can be attributed to the higher energy levels of active particles within the plasma at higher power supply. These energetic particles possess greater momentum, rendering them more effective at interacting with the polyethylene surface and generating additional active groups or free radicals on its surface.

Table 3 displays the gas chromatograph analysis of exhaust gas after DBD treatment. Since the reaction atmosphere consisted of high-purity air composed of 79% N_2 and 21% O_2 , the gas chromatograph analysis results corroborate the findings from the infrared analysis. This confirmation underscores the occurrence of chemical modifications on the polyethylene surface induced by plasma pulses.

Figure 9 illustrates the infrared spectra of polyethylene surfaces treated with DBD at varying supply frequencies. The figure reveals that, following plasma treatment at frequencies of 200, 500, and 800 Hz, new absorption peaks emerge on the polyethylene surface within the range of 1500-1750 cm^{-1} , corresponding to the -C=O functional group. Obviously, the peak intensities remain largely consistent across different frequencies, suggesting that the supply frequency has a minimal impact on the modification of functional groups on the material surface. This observation aligns with the typical discharge properties.

Topographical Changes Induced by DBD: AFM Results. Figure 10 showcases AFM results for polyethylene surfaces treated with DBD for 40 seconds. The experiments maintained a controlled gas flow rate of 5 L/min under experimental air conditions. The untreated polyethylene surface exhibited a root

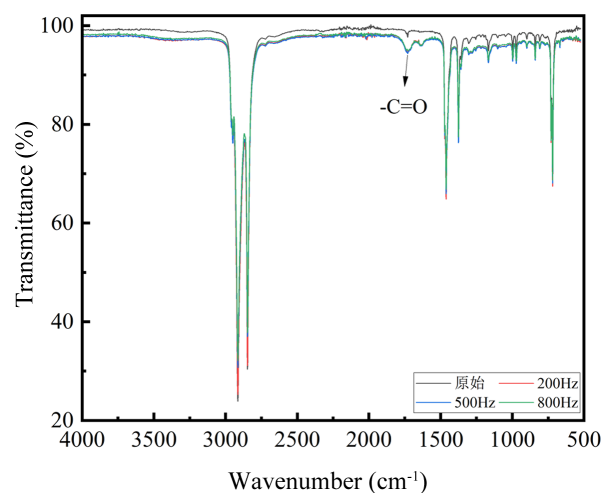


Figure 9. Infrared spectra of polyethylene surfaces after treatment at different frequencies.

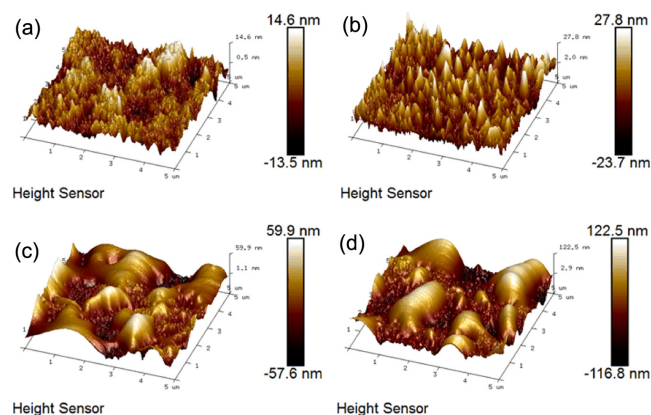


Figure 10. AFM images of polyethylene surfaces treated at different discharge powers: power supply: (a) untreated; (b) 70 W; (c) 108 W; (d) 150 W.

mean square (RMS) value of 3.83nm relative to the reference plane. However, when subjected to discharge powers of 70, 108, and 150 W, the RMS values relative to the reference plane increased to 7.07, 16.8, and 37.9 nm, respectively.

This trend reveals that an increase in power supply leads to the emergence of more surface depressions and protrusions, resulting in a significant rise in surface roughness. This effect signifies that higher power supply levels enhance the material's surface etching by the plasma. The heightened discharge power activates high-energy particles within the gas, intensifying the

Table 3. Gas Chromatograph Analysis of Post-Treatment Exhaust Gas

Degradation Products	H_2	CH_4	C_2H_2	CO	CO_2
Content: (%)	0.0392	0.0002	0.0021	0.4895	1.0621

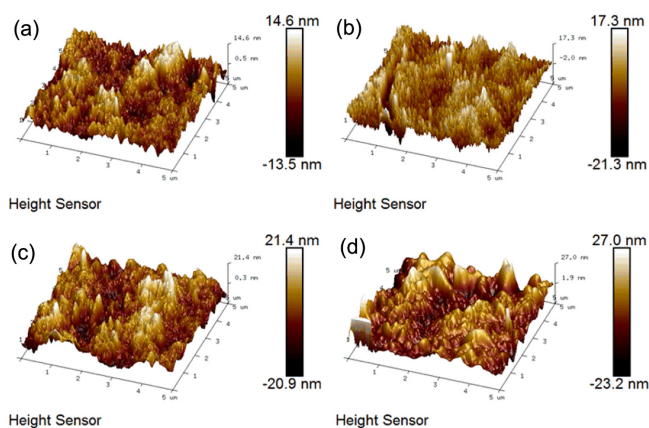


Figure 11. AFM images of polyethylene surfaces treated at different discharge frequencies. supply frequencies: (a) untreated; (b) 200 Hz; (c) 500 Hz; (d) 800 Hz.

momentum of these active particles as they interact with the polyethylene surface, ultimately increasing surface roughness.

In another aspect of our research, the surface treatments were explored at different supply frequencies. As depicted in Figure 11, the untreated polyethylene surface had an RMS value of 3.83 nm relative to the reference plane. When polyethylene surfaces were treated at supply frequencies of 200, 500, and 800 Hz, the corresponding RMS values relative to the reference plane were 5.04, 5.86, and 8.22 nm, respectively. Notably, the treatment effect is considerably weaker than the variations in power supply, reaffirming the consistency in discharge properties: increasing the supply frequency do not enhance the transferring charge or discharge energy.

Moreover, the treated polyethylene surface exhibited a slight increase in roughness with higher supply frequency. This result can be attributed to continuous bombardment on the polyethylene surface by high-energy particles during DBD. These particles either rebounded from the surface or engaged in surface molecular scattering, removing a small number of surface atoms. Concurrently, chemical reactions occurred between active species and the polyethylene surface, resulting in surface etching. Due to the unpredictability of particle impacts during reactions, different areas experienced varying degrees of etching. Some regions received fewer particle impacts, leading to less effective modification and uneven surface topography.

In summary, while an increase in discharge frequency may not boost pulse energy, it does contribute to the improved uniformity of discharge pulses, enhancing treatment effectiveness to some extent.

Effects of DBD on the Hydrophobicity of Polyethylene.

Table 4. Polyethylene Surface WCA Treated at Different Discharge Powers

Powers (W)	Untreated	70	108	150
WCA (°)	91.080	66.880	56.864	35.351

Plasma treatment induces significant alterations in polyethylene's surface properties, impacting its chemistry, topography, and wettability. These changes can be quantified by measuring the WCA. Experimental conditions remained constant with an air flow rate of 5 L/min and a treatment duration of 40 seconds.

In Table 4, experimental findings are presented regarding the water contact angles on plasma-treated polyethylene surfaces at various power supply. Initially, untreated polyethylene displays a WCA of 91.080°, indicating its hydrophobic property. As the power supply increases, the water contact angle gradually diminishes to 35.351°, indicating enhanced hydrophilic modification of polyethylene through increased power supply in the plasma treatment.

The table reveals a substantial reduction in the water contact angle as power supply increases from 108W (56.864°) to 150W (35.351°). This demonstrates a progressive strengthening of the material surface's WCA modification with rising power supply. Consequently, the selection of an appropriate power supply is crucial in experiments, depending on specific circumstances.

Table 5 showcases the experimental findings of WCA on plasma-treated polyethylene surfaces under various discharge frequencies. Notably, an increase in discharge frequency correlates with a gradual reduction in the water contact angle, reaching 60.042°. This indicates that elevating the discharge frequency can moderately enhance the plasma's hydrophilic modification effect on polyethylene.

In Figure 12, an intuitive comparison of two critical power factors is shown on the polyethylene surface. Both power supply and frequency exhibit similar patterns in influencing polyethylene surface modification. As these parameters increase, they enhance the modification effects.

Increasing power supply directly amplifies transferring charge amplitude and intensity, resulting in a more effective WCA modification under identical conditions. Conversely, elevating

Table 5. Polyethylene Surface WCA Treated at Different Discharge Frequencies

Frequencies (Hz)	Untreated	200	500	800
WCA (°)	91.080	76.373	68.378	60.042

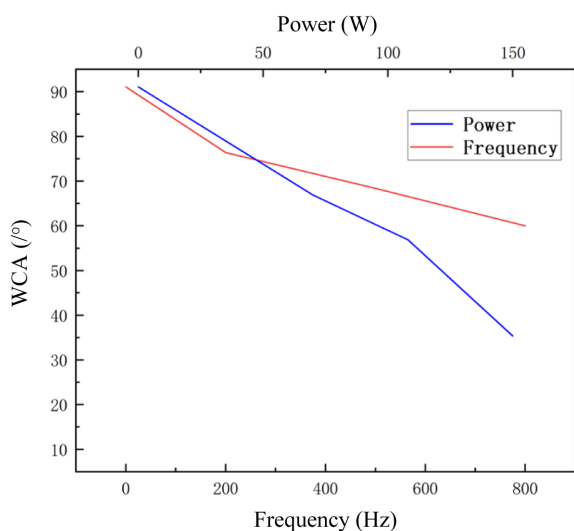


Figure 12. Power and frequency effects on hydrophobicity.

power frequency primarily accelerates reaction rates and promotes discharge uniformity, albeit without directly increasing discharge intensity. Consequently, its impact on modification is limited.

In all hydrophobicity treatments, the optimal conditions for modifying the surface hydrophilicity of polyethylene material were selected, with a power supply of 150 W, to investigate the aging effect of atmospheric pressure low-temperature plasma treatment on polyethylene. The experiments were conducted under the following constant conditions: treatment time of 40 seconds, ambient air, 25 °C, and 40% humidity. The detailed

findings are illustrated in Figure 13 and summarized in Table 6.

Figure 13 showcases images depicting the water contact angles on the polyethylene surface at various time intervals following plasma treatment. These intervals are denoted as (a)–(g) and represent 0, 24, 36, 48, 144, 288, and 720 h, respectively. Table 6 quantifies the corresponding degree of modification loss.

From Figure 13, it can be observed that immediately after plasma treatment, the water contact angle on the polyethylene surface measures 35.351°, indicating a result of hydrophilicity. However, over time, as the material is exposed to air, the WCA gradually rises. After 720 hours, it reaches 86.948°, closely resembling the initial hydrophobic surface at 91.080°. Notably, during the initial phase (0 to 144 hours), the material exhibits the swiftest recovery in WCA, as reflected in Table 6, with a rapid increase from 0% to an overall loss of 61.8%. After 144 hours of air exposure, the rate of WCA recovery on the polyethylene surface decelerates, as indicated in Table 6, with an increase from 61.8 to 92.6%. Eventually, it approaches the hydrophobic surface properties prior to treatment.

This evolution suggests that the plasma-induced modification of the material's surface is not permanent. This is because while DBD serves as an effective method for polymer surface modification, these modified surface properties are susceptible to aging, leading to what is known as “hydrophobic recovery”. This phenomenon manifests as the gradual partial or complete reversion of the modified surface to the original polymer's hydrophobic state with prolonged storage. The occurrence is

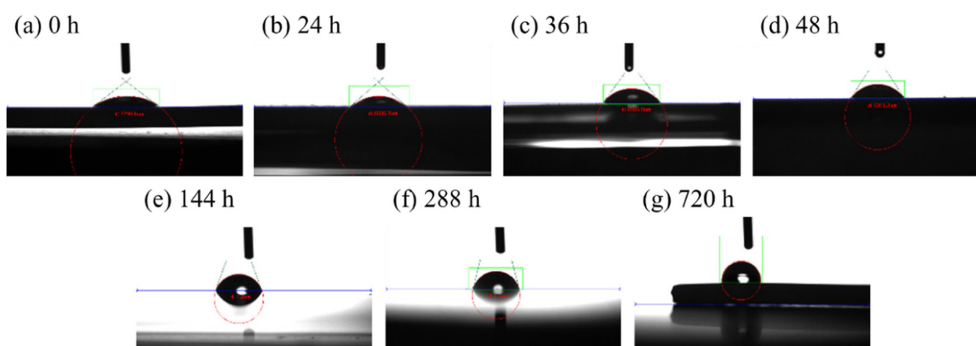


Figure 13. Water contact angle on polyethylene surface at various post-treatment duration of placement: (a) 0 h; (b) 24 h; (c) 36 h; (d) 48 h; (e) 144 h; (f) 288 h; (g) 720 h.

Table 6. Loss Degree of Modification Effect Over Time

Hour (h)	0	24	36	48	144	288	720
WCA (°C)	35.351	41.081	53.964	56.579	69.804	75.628	86.948
Loss (%)	0	10.3	33.4	38.1	61.8	72.3	92.6

rooted in the migration of polar functional groups from the modified polymer surface into the polymer's interior within a non-polar environment. Concurrently, non-polar segments of the polymer relocate to the surface. As a result, the decrease in polar functional groups on the polymer surface and the recovery of unmodified non-polar functional groups diminishes the interfacial energy between the surface and the surroundings. Consequently, this prompts the polymer to tend towards reverting to its initial surface properties.

Conclusions

The DBD properties under different power supply parameters and the corresponding surface modification experimental results were studied, leading to several conclusions:

1. As the power supply increases, the discharge intensity also increases, with the current amplitude and the amplitude of transferring charge per pulse continuously rising.

2. An increase in supply frequency doesn't affect overall discharge intensity but accelerates discharge rates and increases discharge occurrences.

3. Greater power supply induces more pronounced chemical changes on the polyethylene surface due to DBD, while variations in supply frequency have minimal impact.

4. Increasing power supply results in more significant topographical changes on the polyethylene surface through DBD. Although supply frequency changes yield weaker overall treatment effects, the enhanced uniformity of discharge pulses moderately improves treatment effectiveness.

5. With an increase in power supply, DBD induces a progressively stronger alteration in hydrophobicity. In contrast, changes in supply frequency have a comparatively milder impact.

Acknowledgement: The funders had no role in the design of the study; in the collection, analyses, or interpretation of data; in the writing of the manuscript; or in the decision to publish the results. The data will be made available from the corresponding author on reasonable request.

Conflicts of Interest: The authors declare no conflict of interest.

References

1. Rutkuniene, Z.; Pervazaitė, M.; Skirbutis, G., Modification of Polyetheretherketone Surface by Argon, Oxygen and Nitrogen Plasma for Dentistry Application. *Proceeding of the 4th International Conference on Geotechnical Research and Engineering (ICGRE 2019)*, Rome, Italy, April 7-10, 2019; pp 160-164.
2. Chaichi, A.; Prasad, A.; Parambil, L. K.; Shaik, S.; Etefagh, A. H.; Dasa, V.; Guo, S.; Osborn, M. L.; Devireddy, R.; Khonsari, M. M.; Gartia, M. R., Improvement of Tribological and Biocompatibility Properties of Orthopedic Materials Using Piezoelectric Direct Discharge Plasma Surface Modification. *ACS Biomater. Sci. Eng.* **2019**, *5*, 2147-2159.
3. Zhao, Y.; Zhu, B.; Wang, Y.; Liu, C.; Shen, C., Effect of Different Sterilization Methods on the Properties of Commercial Biodegradable Polyesters for Single-use, Disposable Medical Devices. *Mater. Sci. Eng. C* **2019**, *105*, 110041.
4. Fedel, M.; Micheli, V.; Thaler, M.; Awaja, F., Effect of Nitrogen Plasma Treatment on the Crystallinity and Self-bonding of Polyetheretherketone (PEEK) for Biomedical Applications. *Polym. Adv. Technol.* **2020**, *31*, 240-247.
5. Luque-Agudo, V.; Hierro-Oliva, M.; Gallardo-Moreno, A. M.; Luisa Gonzalez-Martin, M., Effect of Plasma Treatment on the Surface Properties of Polylactic Acid Films. *Polym. Test.* **2021**, *96*, 107097.
6. Kovacs, R. L.; Csontos, M.; Gyongyosi, S.; Elek, J.; Parditka, B.; Deak, G.; Kuki, A.; Keki, S.; Erdelyi, Z., Surface Characterization of Plasma-modified Low Density Polyethylene by Attenuated Total Reflectance Fourier-transform Infrared (ATR-FTIR) Spectroscopy Combined with Chemometrics. *Polym. Test.* **2021**, *96*, 107080.
7. Wiacek, A. E.; Terpilowski, K.; Jurak, M.; Wozzakowska, M., Low-temperature Air Plasma Modification of Chitosan-coated PEEK Biomaterials. *Polym. Test.* **2016**, *50*, 325-334.
8. Hegemann, D.; Brunner, H.; Oehr, C., Plasma Treatment of Polymers for Surface and Adhesion Improvement. *Nucl. Instrum. Methods Phys. Res. Sect. B* **2003**, *208*, 281-286.
9. Aawaja, F.; Gilbert, M.; Kelly, G.; Fox, B.; Pigram, P. J., Adhesion of Polymers. *Prog. Polym. Sci.* **2009**, *34*, 948-968.
10. Lommatzsch, U.; Pasedag, D.; Baalman, A.; Ellinghorst, G.; Wagner, H.-E., Atmospheric Pressure Plasma Jet Treatment of Polyethylene Surfaces for Adhesion Improvement. *Plasma Processes Polym.* **2007**, *4*, S1041-S1045.
11. Moraczewski, K.; Stepczynska, M.; Malinowski, R.; Rytlewski, P.; Jagodzinski, B.; Zenkiewicz, M., Stability Studies of Plasma Modification Effects of Polylactide and Polycaprolactone Surface Layers. *Appl. Surf. Sci.* **2016**, *377*, 228-237.
12. Moraczewski, K.; Rytlewski, P.; Malinowski, R.; Zenkiewicz, M., Comparison of Some Effects of Modification of a Polylactide Surface Layer by Chemical, Plasma, and Laser Methods. *Appl. Surf. Sci.* **2015**, *346*, 11-17.
13. Minati, L.; Migliaresi, C.; Lunelli, L.; Viero, G.; Dalla Serre, M.; Speranza, G., Plasma Assisted Surface Treatments of Biomaterials. *Biophys. Chem.* **2017**, *229*, 151-164.
14. Khorasani, M. T.; Mirzadeh, H.; Irani, S., Plasma Surface Modification of Poly(L-lactic acid) and Poly(lactic-co-glycolic acid) Films for Improvement of Nerve Cells Adhesion. *Radiat. Phys. Chem.* **2008**, *77*, 280-287.
15. Goddard, J. M.; Hotchkiss, J. H., Polymer Surface Modification

- for the Attachment of Bioactive Compounds. *Prog. Polym. Sci.* **2007**, *32*, 698-725.
16. Yoshida, S.; Hagiwara, K.; Hasebe, T.; Hotta, A., Surface Modification of Polymers by Plasma Treatments for the Enhancement of Biocompatibility and Controlled Drug Release. *Surf. Coat. Technol.* **2013**, *233*, 99-107.
17. Bui, V.-T.; Liu, X.; Ko, S. H.; Choi, H.-S., Super-amphiphilic Surface of Nano Silica/polyurethane Hybrid Coated PET Film via a Plasma Treatment. *J. Colloid Interface Sci.* **2015**, *453*, 209-215.
18. Thakur, S.; Pal, D.; Neogi, S., Prevention of Biofilm Attachment by Plasma Treatment of Polyethylene. *Surf. Innovations* **2016**, *4*, 33-38.
19. Suganya, A.; Shanmugavelayutham, G.; Serra Rodriguez, C., Study on Structural, Morphological and Thermal Properties of Surface Modified Polyvinylchloride (PVC) Film Under Air, Argon and Oxygen Discharge Plasma. *Mater. Res. Express* **2016**, *3*, 095302.
20. Sonmez, T.; Jadidi, M. F.; Kazmanli, K.; Birer, O.; Urgen, M., Role of Different Plasma Gases on the Surface Chemistry and Wettability of RF Plasma Treated Stainless Steel. *Vacuum* **2016**, *129*, 63-73.
21. Shafei, S.; Foroughi, J.; Chen, Z. Q.; Wong, C. S.; Naebe, M., Short Oxygen Plasma Treatment Leading to Long-Term Hydrophilicity of Conductive PCL-PPy Nanofiber Scaffolds. *Polymers* **2017**, *9*, 614.
22. Mandolino, C.; Lertora, E.; Gambaro, C.; Pizzorni, M., Functionalization of Neutral Polypropylene by Using Low Pressure Plasma Treatment: Effects on Surface Characteristics and Adhesion Properties. *Polymers* **2019**, *11*, 202.
23. Lin, F. B.; Li, W.; Tang, Y.; Shao, H. Q.; Su, C. L.; Jiang, J. H.; Chen, N. L., High-Performance Polyimide Filaments and Composites Improved by O₂ Plasma Treatment. *Polymers* **2018**, *10*, 695.
24. Zaplotnik, R.; Vesel, A., Effect of VUV Radiation on Surface Modification of Polystyrene Exposed to Atmospheric Pressure Plasma Jet. *Polymers* **2020**, *12*, 1136.
25. Wu, Y. Q.; Ding, L. J.; Zhang, C.; Shao, T.; Chen, W. J., Experimental Study on the Treatment of Oil-based Drill Cutting by Pulsed Dielectric Barrier Discharge Plasma at Atmospheric Pressure. *J. Cleaner Prod.* **2022**, *339*, 130757.
26. Feitor, M. C.; Aves Junior, C.; Bezerra, C. M.; Magalhoes de Sousa, R. R.; de Carvalho Costa, T. H., Evaluation of Aging in Air of Poly(Ethylene Terephthalat) in Oxygen Plasma. *Mater. Res.-Ibero-am. J. Mater.* **2015**, *18*, 891-896.
27. Buzi, L.; Miyazoe, H.; Sagianis, M. P.; Marchack, N.; Papalia, J. M.; Engelmann, S. U., Utilizing Photosensitive Polymers to Evaluate UV Radiation Exposures in Different Plasma Chamber Configurations. *J. Vac. Sci. Technol. A* **2020**, *38*, 033006.
28. Morent, R.; De Geyter, N.; Trentesaux, M.; Gengembre, L.; Dubruel, P.; Leys, C.; Payen, E., Influence of Discharge Atmosphere on the Ageing Behaviour of Plasma-Treated Poly(lactic Acid). *Plasma Chem. Plasma Process.* **2010**, *30*, 525-536.
29. Izdebska-Podsiadly, J.; Doersam, E., Effects of Argon Low Temperature Plasma on PLA Film Surface and Aging Behaviors. *Vacuum* **2017**, *145*, 278-284.
30. Jovanovic, O.; Puac, N.; Skoro, N., A Comparison of Power Measurement Techniques and Electrical Characterization of An Atmospheric Pressure Plasma Jet. *Plasma Sci. Technol.* **2022**, *24*, 105404.
31. Zheng, H.; Liang, H.; Chen, J.; Zong, H. H.; Meng, X. Z.; Xie, L. K.; Li, Y. H., Experimental Study on Plasma Actuation Characteristics of Nanosecond Pulsed Dielectric Barrier Discharge. *Plasma Sci. Technol.* **2022**, *24*, 015505.
32. Wang, R. X.; Yang, Y. W.; Chen, S. B.; Jiang, H.; Martin, P., Power Calculation of Pulse Power-Driven DBD Plasma. *IEEE Trans. Plasma Sci.* **2021**, *49*, 2210-2216.
33. Wilde, N. D.; Xu, H. F.; Gomez-Vega, N.; Barrett, S. R. H., A Model of Surface Dielectric Barrier Discharge Power. *Appl. Phys. Lett.* **2021**, *118*, 154102.
34. Fan, R.; Wang, Y. G.; Liu, Y.; Zhang, X. N.; Tu, Z. T.; Zhang, J., The Exploration of Discharge Efficiency and Uniformity Improvement with Pre-ionized Bipolar Pulse Method in DBD Device. *Phys. Plasmas* **2020**, *27*, 083508.
35. Rad, Z. S.; Davani, F. A., Experimental Investigation on Electrical Characteristics and Dose Measurement of Dielectric Barrier Discharge Plasma Device Used for Therapeutic Application. *Rev. Sci. Instrum.* **2017**, *88*, 043504.
36. Jiang, H.; Shao, T.; Zhang, C.; Li, W.; Yan, P.; Che, X.; Schamiloglu, E., Experimental Study of Q-V Lissajous Figures in Nanosecond-Pulse Surface Discharges. *IEEE Trans. Dielectr. Electr. Insul.* **2013**, *20*, 1101-1111.
37. Biganzoli, I.; Barni, R.; Gurioli, A.; Pertile, R.; Riccardi, C., Experimental Investigation of Lissajous Figure Shapes in Planar and Surface Dielectric Barrier Discharges. *J. Phys. Conf. Ser.* **2014**, *550*, 012039.
38. Akamatsu, H.; Ichikawa, K., Characteristics of Atmospheric Pressure Plasma Jet Generated by Compact and Inexpensive High Voltage Modulator. *Surf. Coat. Technol.* **2011**, *206*, 920-924.
39. Ahmed, K. M.; Allam, T. M.; El-sayed, H. A.; Soliman, H. M.; Ward, S. A.; Saied, E. M., Design, Construction and Characterization of AC Atmospheric Pressure Air Non-thermal Plasma Jet. *J. Fusion Energy* **2014**, *33*, 627-633.

Publisher's Note The Polymer Society of Korea remains neutral with regard to jurisdictional claims in published articles and institutional affiliations.